Direct Gray Scale Ridge Reconstruction in Fingerprint Images

Carlotta Domeniconi Sibel Tari Ping Liang
Electrical Engineering Department
University of California
Riverside, CA 92521

Abstract[1]

An original technique, based on ridge point detection directly from gray scale fingerprint images, is proposed. Our method avoids serious problems that algorithms which perform binarization of fingerprint images have. Each step can be easily hardware implemented, allowing a relevant speed up of the whole process.

Keywords: Fingerprints, gray scale images, minutiae, feature extraction.

1 Introduction

Automated identification of fingerprints is a difficult problem with many important applications. Many Automated Fingerprint Identification Systems (AFIS) are already in use in law enforcement applications. However, the technology is still developing and there are still many unsolved research problems [4].

The inner surface of a finger is covered with a pattern of friction ridges. Most fingerprint recognition algorithms are typically based on extraction of specific feature points, called minutiae points, located on ridges [1]. As highlighted in the lower image of Figure 6, a minutia point is defined as the location where a single ridge bifurcates into two ridges or where a ridge ends. Other features besides minutiae points are frequently used to classify fingerprints so they can be filed for future retrieval [3]. In AFIS all fingerprints with the same classification are searched for a match with the input fingerprint. This step is called the print-to-print search, i.e., search for a matching of fingerprints to determine if they come from the same finger of an individual. The print-to-print search compares two fingerprint images directly or compares features extracted from the input fingerprint image with features extracted from fingerprint images in the database.

Several approaches have been proposed in the literature; although rather different from each other, all these methods transform fingerprint images into binary images [7, 6]. The main difficulty of this approach is due to the fact that fingerprints quality is often too low, and when binarization is applied to noisy and low-contrast images often produces unsatisfactory results. Noise and contrast deficiency can produce false minutiae, which are impossible to detect performing local analysis, and hide valid ones. Moreover, the binarization process may cause the loss of a significant amount of information, it requires the setting of critical threshold values, and it is time consuming.

Recently Maio et al. addressed the detection of ridges directly from gray scale images. The ridge line following algorithm reported in [5] attempts to locate local maxima relative to a section orthogonal to the ridge direction, resulting in highly complicated implementation which involves seven independent parameters whose values are quite critical.

In this paper we propose an original technique for direct gray scale fingerprint ridge detection. Our basic idea is to view ridge lines as a sequence of maximum and saddle points. Each step can be easily hardware implemented, allowing a relevant speed up of the whole feature extraction process.

2 Ridge Points Detection

Mathematically, ridge points are local maxima along the direction of one of the principal curvature and they are points where the other principal curvature is zero. Figure 1 shows an ideal ridge.

An obvious way to detect ridge points is to examine the second derivatives. Let H denote the hessian matrix at a stationary point p. Let λ_1 and λ_2 , such that $|\lambda_1| \geq |\lambda_2|$, be the characteristic values of H. If p is a ridge point then $\lambda_1 < \lambda_2 = 0$.

Detection of ridge points is not stable. Slight perturbations due to various factors (e.g. *noise, discretization grid size*) may change zero eigenvalues to non-zero values. A point which satisfies the previous

[1]E-mail: carlotta@ee.ucr.edu, stari@ee.ucr.edu, liang@ee.ucr.edu. Research is in part funded by the TRW fund of the Cleveland foundation.
In Proceedings of ICASSP '98.

condition at a given resolution, may not satisfy the same condition at a higher resolution. In general, our "ideal" ridges will change into a sequence of local maxima and saddle points. See Figure 2. Hence it is appropriate to search for such a general pattern rather than the idealized ridges of Figure 1. A stationary point p is a local maximum iff

$$\lambda_1 \leq \lambda_2 < 0. \tag{1}$$

A stationary point p is a saddle point iff

$$\lambda_1 \lambda_2 < 0.$$

To distinguish saddle points which are on a ridge from those which are on a valley, we consider only the ones which are local maxima in the direction of maximum change and local minima in the direction of minimum change. Thus we establish that a stationary point p is a saddle point iff

$$\begin{aligned} \lambda_1 &< 0 \\ \lambda_2 &> 0. \end{aligned} \tag{2}$$

Ridge pixels may gradually change their intensity values along the ridge direction, causing the surface to have positive or negative slope. This phenomenon is evident near ridges endings, as Figure 2 shows. Figure 3 shows the zero-crossings of the x and y components of the gradient of a small area of a fingerprint shown in Figure 4. The intersection points between the two zero levels correspond to the simultaneous zero-crossings of the x and y gradient components, hence to the stationary points. Ridge's branches with positive or negative slope have no stationary points. Figure 5 shows the plot of the gradient vectors which correspond to the portion of a ridge. The branch of the ridge with no zero-crossing points is highlighted with a circle. Pixels on this branch are still maximum points along the orthogonal direction.

Let p be a point on a ridge which is not a stationary point. Let p_1 and p_2 be the two neighbors of p along the direction orthogonal to the ridge. Let $\vec{n}_1$ and $\vec{n}_2$ denote the gradient vectors at pixels p_1 and p_2. Since p is a maximum point along the orthogonal direction, the gradient vectors $\vec{n}_1$ and $\vec{n}_2$ point at opposite directions:

$$\frac{\vec{n}_1}{|\vec{n}_1|} \cdot \frac{\vec{n}_2}{|\vec{n}_2|} = \cos(\pi) = -1 \tag{3}$$

In real cases, equation (3) may never be satisfied due to the presence of noise. As a consequence, $\vec{n}_1$ and $\vec{n}_2$ will have directions which are "almost" opposite (see Figure 5). This pattern is searched for non stationary points. The second derivatives are investigated also for those points, in order to determine which of them belong to ridges and which of them to valleys. Same criteria as in (1) and (2) are applied. A point p whose neighbors satisfy condition (3) is a ridge point situated on a negative slope iff condition (1) applies. A point p whose neighbors satisfy condition (3) is a ridge point situated on a positive slope iff condition (2) applies.

It is important to underline that using gradient direction for ridge detection is quite stable, whereas selecting ridge points by setting a threshold on the absolute value of the gradient is not a robust condition. This is because the appropriate threshold may change from image to image, or even from area to area within the same image. All our conditions are based on properties of the intensity surfaces of the gray scale fingerprint images. Those properties are direct consequences of the nature of the fingerprint images.

3 Implementation

Let $I_x = \frac{\partial I}{\partial x}$ and $I_y = \frac{\partial I}{\partial y}$. We detect the stationary points as the simultaneos zero-crossings of I_x and I_y. We also consider non stationary points which satisfy condition (3). In our experiments we use the value $\frac{5}{9}\pi$ for the angle between $\vec{n}_1$ and $\vec{n}_2$. Hessian matrix is computed at each selected point using central differences. H is a 2×2 real symmetric matrix. Thus calculation of the eigenvalues is trivial. The roots of the characteristic polynomial, which is a second degree polynomial, directly give the eigenvalues. Once the eigenvalues are computed points on ridges are easily determined using (1) and (2).

Fingerprint images may be very noisy, especially those acquired by ink technique. Thus it is appropriate to smooth the image prior to ridge point extraction. We smooth the image using geometric heat equation, by applying gradient descent to the functional $\int\int |\nabla I| dxdy$. Since we do not attempt to perform binarization, degree of smoothing is not extremely critical. Still we avoid using smoothing tools such as convolution with a Gaussian kernel which is equivalent to isotropic diffusion equation. Such non-selective smoothing tends to smear out the ridges. Geometric heat equation provides a good enough smoothing while preserving the ridges, and it is invariant with respect to contrast.

The upper image of Figure 6 shows the result of ridge point detection on a sample fingerprint image classified as a poor quality image [2]. The original fingerprint image, which belongs to NIST Special Database 4 [8], is shown in the lower image of Figure 6.

4 Ridge Reconstruction Algorithm

Previous sections presented an easy and robust technique for finding ridge points. In this section we address how to use the ridge points to perform ridge reconstruction. The purpose of our ridge reconstruction algorithm is to collect and organize, in meaningful structures, the detected ridge points which are connected and to properly recover, if present, the gaps between them. The resulting structures correspond to our representation of fingerprint images which can be directly used to address the print-to-print matching problem. Our ridge reconstruction algorithm is completely driven by the points already detected. No ridge following algorithm based on gradient information is performed, since ridge points are available. Each branch of connected points is traced only once starting from one of its ending point. Once the opposite ending point is reached, minimum squared error (*mse*) line fitting is performed at both endings, to determine the directions along which move forward to look for other nearby branches. If a branch not traced yet is found, gap is filled with points and tracing of connected points continues; if a branch of a ridge already traced is encountered the gap is filled with points and the two branches are merged. When all branches of connected points are traced the algorithm stops. All merged branches belong to the same data structure which is stored in memory.

The result of the ridge reconstruction algorithm applied on points shown in the upper image of Figure 6 is shown in the middle image of the same Figure. In this case 20 points or at least 4 points (if 20 points are not available on the branch which is currently traced) are used, when performing *mse* line fitting, and 6 pixels is the distance recovered along the tangent direction given by the *mse* line fitting. The algorithm is able to recover most of the breaks between branches belonging to the same ridge. Moreover, the algorithm is able, almost always, to avoid false connections which can arise on account of the presence of noise across ridges. False connections due to the presence of noise across ridges are a serious problem of algorithms which perform binarization of fingerprint images. Our algorithm is able to avoid this problem not allowing gap filling if the branch of connected points which has been traced is too short (less than 4 pixels in our experiments). A short branch which is not merged with other branches can be easily removed during a post processing phase.

5 Conclusions and Future Work

For the print-to-print matching problem, bifurcation and end points extraction can easily be performed directly on the image resulting from our ridge reconstruction algorithm. A post processing stage can eliminate spurious feature points, which may be still present, based on the structural and spatial relationships of the minutiae. For instance, two minutiae in a real fingerprint cannot occur within a distance of few pixels from each other. Proper heuristics can be implemented to perform ridge break and spike elimination. Two end points with the same orientation and within a distance threshold can be eliminated; an end point which is connected to a bifurcation point and is also within a distance threshold can be eliminated.

The resulting ridges form a template which carries information, such as curvature of ridges, length of ridges, spatial frequencies, orientation, which may be used to address the print-to-print matching problem, directly without performing feature points extraction.

These ideas will be further investigated in order to efficiently solve the print-to-print matching problem.

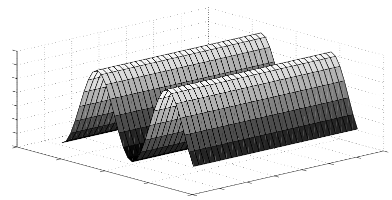

Figure 1: Ideal ridge surface.

References

[1] U.S. Dept. of Justice, The Science of Fingerprint, 1984, Washington D.C..

[2] Donahue, M.J., and Rokhlin, S.I., 1993, "On the Use of Level Curves in Image Analysis", *Image Understanding*, Vol. **57**, No. 2, pp. 185–203.

[3] Karu, K., and Jain, A.K., 1996, "Fingerprint Classification", *Pattern Recognition*, Vol. **29**, No. 3, pp. 389–404.

[4] Langley, R.J., 1995, "An Introduction to Automated Fingerprint Identification Systems", *Technology Review, TRW Systems Integration Group*, Vol. **3**, No. 2, pp. 3–27.

[5] Maio, D., and Maltoni, D., 1997, "Direct Gray-Scale Minutiae Detection In Fingerprint", *IEEE Trans. on Pattern Analysis and Machine Intelligence*, Vol. **19**, No. 1, pp. 27–40.

[6] Ratha, N.K., Chen, S., and Jain, A.K., 1995, "Adaptive Flow Orientation-Based Feature Extraction in Fingerprint Images", *Pattern Recognition*, Vol. **28**, No. 11, pp. 1657–1672.

[7] Ratha, N.K., Karu, K., N.K., Chen, S., and Jain, A.K., 1996, "A Real-Time Matching System for Large Fingerprint Databases", *IEEE Trans. on Pattern Analysis and Machine Intelligence*, Vol. **18**, No. 8, pp. 799–813.

[8] Watson, C.I., and Wilson, C.L., 1992, NIST Special Database 4, Fingerprint Database, National Institute of Standards and Technology.

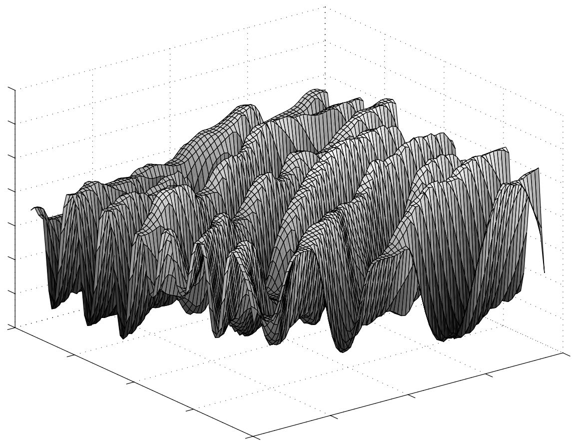

Figure 2: Surface corresponding to a small area of a fingerprint. It shows how our "ideal" ridges change into a sequence of local maxima and saddle points.

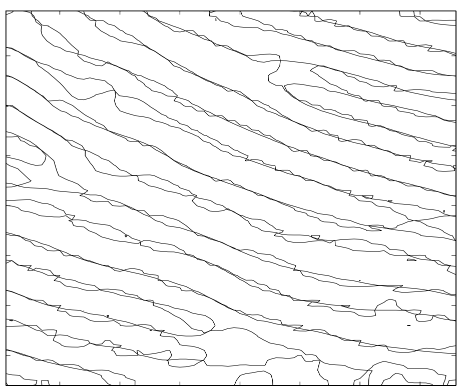

Figure 3: Zero-crossings of the x and y components of the gradient corresponding to a small area of a fingerprint.

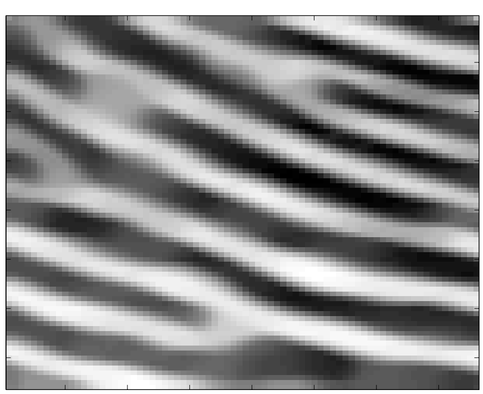

Figure 4: Small area of a fingerprint.

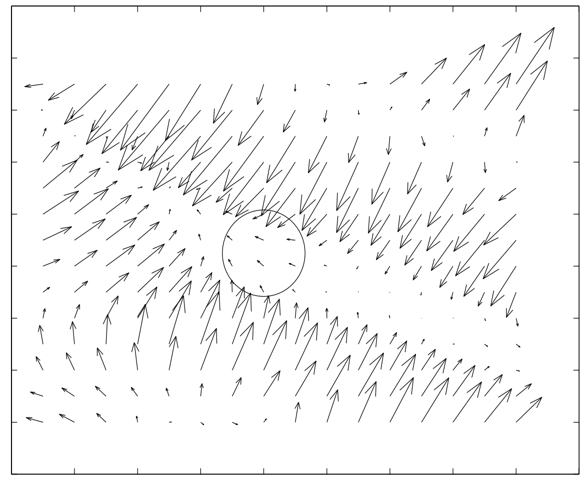

Figure 5: Gradient vectors corresponding to a portion of a ridge.

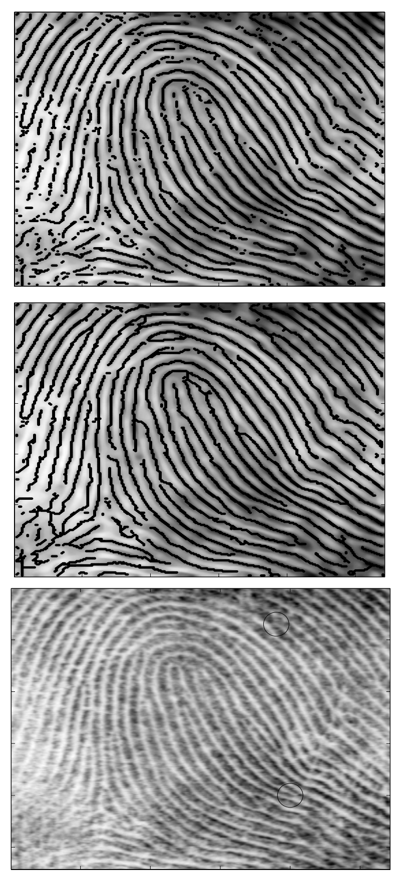

Figure 6: Upper image: result of ridge point detection. Middle image: result of ridge reconstruction. Lower image: original sample image (NIST Special Database 4). Bifurcation and end points are highlighted.